energy&fuels

Article

Cite This: *Energy Fuels* 2018, 32, 8483−8493

pubs.acs.org/EF

Assessment of Hydrotreatment for Hydrothermal Liquefaction Biocrudes from Sewage Sludge, Microalgae, and Pine Feedstocks

Jacqueline M. Jarvis,[†] Karl O. Albrecht,[‡] Justin M. Billing,[‡] Andrew J. Schmidt,[‡] Richard T. Hallen,[‡] and Tanner M. Schaub*,[†]

[†]Chemical Analysis and Instrumentation Laboratory, College of Agriculture, Consumer and Environmental Sciences, New Mexico State University, 945 College Avenue, Las Cruces, New Mexico 88003, United States

[‡]Chemical and Biological Processes Development Group, Pacific Northwest National Laboratory, P.O. Box 999, Richland, Washington 99352, United States

Supporting Information

Downloaded via UNIV OF NEW MEXICO on December 20, 2018 at 15:09:57 (UTC).
See https://pubs.acs.org/sharingguidelines for options on how to legitimately share published articles.

ABSTRACT: Bulk property measurement, simulated distillation, gas chromatography mass spectrometry (GC-MS), and ultra-high-resolution Fourier transform ion cyclotron resonance mass spectrometry (FT-ICR MS) are utilized for direct description and comparison of the chemical composition of raw and hydrotreated biocrude samples from pine, microalgae (*Chlorella* sp.), and sewage sludge. With hydrotreatment, the nitrogen, oxygen, and sulfur content as well as viscosity, density, and moisture content of all biocrudes decreased to yield a more desirable product. For upgraded biocrudes, simulated distillation and GC-MS data reveal that the microalgae and sewage sludge products comprise a high proportion of *n*-alkanes, which distill between 260 and 350 °C, whereas the pine hydrotreated biocrude product has a lower concentration of *n*-alkanes and is more compositionally diverse with an abundance of saturated cyclic compounds. FT-ICR MS analysis of the raw biocrudes showed predominantly O_x species, whereas raw microalgae and sewage sludge biocrudes comprise primarily N_xO_y species. After hydrotreatment, FT-ICR mass spectra of all three biocrudes revealed a significant reduction in mass spectral complexity (observed as the loss of O_x, N_x, and N_xO_y species) and the formation of hydrocarbon compounds, as expected. The hydrodeoxygenation and hydrodenitrogenation reactions of hydrotreatment convert higher (>2) heteroatom-containing species to a variety of hydrocarbon and lower heteroatom-containing species.

INTRODUCTION

The identification of renewable liquid transportation fuels is of enormous public interest in recent years, and a heavy focus has been devoted to biomass as a partial replacement for petroleum crude oil. Hydrothermal liquefaction (HTL) has developed as one of the most promising thermochemical processes for the conversion of wet biomass into transportation fuels.[1−3] Through HTL, increased temperature (250−375 °C) and pressure (4−22 MPa) convert a biomass slurry (∼5−35% solids in water) into a hydrocarbon-rich product.[1] Because HTL requires a pumpable biomass slurry, HTL is especially advantageous (economically) for the conversion of wet biomass because there is limited need for water removal prior to biomass conversion.[1,4] In some cases, water recovery and/or recycle makes HTL of low moisture feeds (e.g., lignocellulose) feasible.[1] Therefore, a range of biomass feedstocks (e.g., lignocellulose, algae, waste products) can be subjected to HTL processes to generate potential biofuels.[5−10]

Biocrudes generated by HTL have generally high heteroatom content, a property that causes HTL biocrudes to be immiscible with typical petroleum crude oils and therefore incompatible with conventional petroleum refinery equipment and processes. Furthermore, the high heteroatom content (and the presence of metals in some cases) of raw HTL biocrudes poisons catalysts used for denitrogenation/desulfurization and catalytic cracking of petroleum crude oils. Consequently, raw HTL biocrudes must undergo some form of upgrading before they can be used as a feasible amendment to conventional petroleum crude oil refinery inputs.

Biocrude upgrading through catalytic hydrotreatment is promising for the conversion of polar compounds into hydrocarbon-rich mixtures with fewer heteroatom-containing species. During hydrotreatment, hydrogen (35−170 bar H_2) and heterogeneous catalysts (e.g., sulfided Co−Mo, Ni−Mo) are used to upgrade raw biocrude at high temperature (300−450 °C) and at a liquid hourly space velocity of 0.2−10 h^{-1}.[11] Catalytic hydrodeoxygenation, hydrodesulfurization, and hydrodenitrogenation are required to remove the high oxygen (5−18 wt %), sulfur (0.5−1.0 wt %), and nitrogen contents (0.3−8 wt %) characteristic of the biocrudes produced by certain feedstocks such as microalgae and waste products.[1] Hydrotreated HTL biocrudes may be fractionated to boiling fractions analogous to those of gasoline, diesel, and/or fuel oil and blended with petroleum products or further refined to create a neat on-spec fuel.

Mass spectrometry has been extensively utilized to identify the compounds within conventional and nonconventional crude oils. Low molecular weight, volatile organics are accessible to gas chromatography mass spectrometry (GC-MS) and can be easily identified by GC-MS techniques.[12−14] However, the complexity exhibited by higher molecular weight,

Received: April 23, 2018
Revised: June 19, 2018
Published: June 30, 2018

ACS Publications © 2018 American Chemical Society

DOI: 10.1021/acs.energyfuels.8b01445
Energy Fuels 2018, 32, 8483−8493

nonvolatile organic species often requires the mass resolving power and high mass accuracy afforded by Fourier transform ion cyclotron resonance mass spectrometry (FT-ICR MS) to obtain a more comprehensive picture of the chemical makeup of crude oils.[15−21] Online and offline separation of organic species can further enhance the information obtained through FT-ICR MS analyses.[22−25] The data obtained through FT-ICR MS analysis have created the field of petroleomics, which can be used to predict both value and behavior of crude oils.[15,18−21,25−27] Previously, a petroleomics approach has been used successfully to determine the chemical composition of raw and upgraded HTL biocrudes and to identify trouble compounds during upgrading.[27−34] Here, we apply the petroleomics approach combined with the data obtained from bulk property measurement, simulated distillation, and GC-MS to give a comprehensive analysis of the chemical composition of raw and hydrotreated HTL biocrudes from pine, microalgae, and sewage sludge to interrogate the feasibility of each feedstock as a potential alternative fuel source. We choose biomass feedstocks that are of recent interest to the field (i.e., lignocellulosic, microalgae, sewage waste) to provide analysis of hydrotreated biocrudes from feeds with variable composition and economic value.[10,35−37]

■ METHODS

Samples. Biocrude samples were obtained from the hydrothermal liquefaction of a clean pine, microalgae (*Chlorella* sp.), and sewage sludge performed at Pacific Northwest National Laboratory (PNNL). Biocrude samples were prepared using bench-scale, continuous-flow process equipment that has been previously described.[2,37] The organic biocrude samples were recovered as a separate phase from the aqueous product. No solvents were used for product recovery. The clean pine feedstock was obtained as wood flour from Idaho National Laboratory. *Chlorella* sp. feedstock was obtained from Global Algae Innovations (http://www.globalgae.com). The sewage sludge biocrude sample was prepared from primary sewage sludge provided by Metro Vancouver wastewater treatment plant.[37,38]

The separated biocrude samples were hydrotreated in a continuous trickle-bed reactor previously described by Elliott et al.[39] following the sulfiding and testing procedure described in Jarvis et al.[30] Briefly, a catalyst composed of 3.4−4.5% cobalt oxide and 11.5−14.5% molybdenum oxide on alumina purchased from Alfa Aesar (Ward Hill, MA, USA; product no. 45579) was employed. The hydrotreatment was conducted at nominally 400 °C and 1500−1540 psig total pressure. Similar to the work of Jarvis et al.,[30] a guard bed of the catalyst in the as-received form of 2.5 mm Trilobe extrudates was employed in the reactor above the catalyst bed. The catalyst bed was composed of catalyst sized to +20/−40 mesh below the guard bed. Table 1 contains the size of the beds as well as the flow rates of the biocrude and H_2 fed to the reactor during hydrotreatment for each of the processed organic biocrudes.

Analysis of Biocrude and Hydrotreated Product. ALS Environmental (Tucson, AZ) conducted elemental analyses for the biomass feed as well as the raw and hydrotreated biocrude liquid according to ASTM D5291/D5373 (for carbon, hydrogen, and nitrogen), ASTM D5373, modified (for oxygen), and ASTMD1552/D4239 (for sulfur). In biocrude oil samples, moisture was determined by the Karl Fischer technique using method ASTM D6869, and total acid number (TAN) was measured following ASTM D3339. The filtered oil solids were measured using ASTM D7579-09, and density and kinematic viscosity measurements were performed at 40 °C using an Anton Paar SVM3000 Stabinger viscometer. Analyses for ash, dry solid content, and product weight were performed gravimetrically. The hydrotreated organic products were analyzed via simulated distillation according to ASTM D2887 and total sulfur analysis following ASTM D5453. The constituents of the hydrotreated organic phases were also analyzed by GC-MS using an Agilent 6890 GC with a 5973 MSD. A 0.1 μL neat sample was injected into a split injector at 280 °C with an 800:1 split ratio using He as a carrier gas at a constant flow of 35 cm/s. A DB1 10 m × 0.1 mm × 0.17 μm column was used. The oven was set at 35 °C with a 2 min hold, followed by a ramp of 10 °C/min to 280 °C with a 5 min hold. The MSD was operated in 70 eV EI mode with a 230 °C source temperature scanning from 16 to 200 m/z until 1.8 min into the method, followed by a scan of 40−600 m/z for the remainder of the method. The GC-MS fragment ion mass spectra were searched against the NIST library for identification of known volatile and semivolatile compounds.

Sample Preparation and Ionization for FT-ICR Mass Spectrometry. Biocrudes were dissolved in 1:1 chloroform/methanol (HPLC grade, JT Baker, Phillipsburg, NJ) to create 1 mg/mL stock solutions. Stock solutions were diluted to a final sample concentration of 100 μg/mL in 90:10 methanol/toluene (biocrudes) for positive-ion atmospheric pressure photoionization.

Atmospheric pressure photoionization (APPI) was performed with an Ion Max APPI source (ThermoFisher Corp., San Jose, CA). Samples were introduced to the source through a fused silica capillary at a rate of 50 μL/min. Nitrogen was used as a sheath gas (60 psi) and auxiliary gas (4 L/min). Inside the heated vaporizer of the source (∼300 °C), the sample is mixed with a nebulization gas (N_2) and is passed under a krypton VUV lamp producing 10 eV photons (120 nm). Toluene was added to the samples to increase ionization efficiency through dopant-assisted photoionization.

FT-ICR Mass Spectrometry. Samples were analyzed with a custom-built 9.4 T Fourier transform ion cyclotron resonance mass spectrometer at the national FT-ICR MS user facility at the National High Magnetic Field Laboratory.[40] Data collection was facilitated by a modular ICR data acquisition system (PREDATOR).[41] Ions generated at atmospheric pressure were introduced into the mass spectrometer via a heated metal capillary. Ions were guided through the skimmer region and quadrupole (mass transfer mode) for accumulation in the second octopole. Finally, ions were collisionally cooled with helium gas (∼(4−5) × 10^{-6} Torr at gauge) before passage through a transfer octopole to the ICR cell (open cylindrical Penning trap[42]).

Multiple (50) individual time-domain transients were coadded, Hanning-apodized, zero-filled, and fast-Fourier-transformed prior to frequency conversion to mass-to-charge ratio[43] to obtain the final mass spectrum. The time domain signal acquisition period was 5.6−6.9 s. All observed ions were singly charged, as evident from unit m/z spacing between species, which differs by $^{12}C_c$ versus $^{13}C_1{}^{12}C_{c-1}$.

Data Analysis and Visualization. Mass spectral lists were generated with PetroOrg software.[44] Internal calibration of the spectrum was based on homologous series whose elemental compositions differ by integer multiples of 14.01565 Da (i.e., CH_2).[45] Data are visualized by relative abundance histograms for heteroatom classes with greater than 1% relative abundance and from isoabundance-contoured plots of double bond equivalents (DBE = number of rings plus double bonds to carbon) versus carbon number for members of a single heteroatom class. The relative abundance scale in isoabundance-contoured plots is scaled relative to the most abundant species in the mass spectrum unless denoted otherwise.

Within the isoabundance-contoured plots, species with DBE ≥ 4 (i.e., benzene ring has a DBE value of 4) are typically considered aromatic, and increases in DBE are correlated to increasing

Table 1. Parameters Employed for the Hydrotreatment of Pine, Microalgae, and Sewage Sludge Biocrudes

	pine	microalgae	sewage sludge
top bed (2.5 mm Trilobe extrudates), cm^3(g)	6 (2.7)	23 (13.1)	6 (3.70)
bottom bed (+20/−40 mesh), cm^3 (g)	39 (25.0)	28 (18.6)	18 (10.8)
biocrude flow rate, cm^3/h	8.02	5.06	4.01
H_2 flow rate, cm^3 H_2/cm^3 biocrude	1230	1276	1276

DOI: 10.1021/acs.energyfuels.8b01445
Energy Fuels 2018, 32, 8483−8493

Table 2. Properties of Raw and Hydrotreated HTL Biocrudes Derived from Pine, Microalgae, and Sewage Sludge Feedstocks

	pine		microalgae		sewage sludge	
	raw	hydrotreated	raw	hydrotreated	raw	hydrotreated
carbon (wt %)	83	87	79	86	77	84
hydrogen (wt %)	6.7	11	11	15	10	15
oxygen (wt %)	10	2.0	3.1	1.2	8.4[a]	1.2
nitrogen (wt %)	0.18	<0.05	5.5	<0.05	4.3	0.05
sulfur (wt % or ppm)	<0.03	46 ppm	0.6	17 ppm	0.63	23 ppm
H/C (mol ratio)	0.97	1.6	1.6	2.1	1.6	2.0
TAN (mg KOH/g oil)[b]	53	N/D[b]	53	N/D	65	<0.01
density (g/mL)	1.1	0.90	0.96	0.78	1.0	0.79
viscosity (cSt@40 °C)	>10000	4.5	295	2.2	571	2.5
moisture (wt %)	16.9	<0.3	12.0	<0.2	13.0	<0.1
ash (wt %)	0.07	N/D	0.47	N/D	0.33	N/D
filterable solids (wt %)	0.04	N/D	0.36	N/D	0.18	N/D

[a]Oxygen determined by difference. [b]Not determined.

aromaticity (i.e., additional aromatic rings increase by 3 DBE). Double bonds and rings also increase DBE value, so it is possible that increases in DBE do not correspond to increasing aromaticity. However, from what is known about the chemical structure and reaction chemistry of biocrudes,[46] it is unlikely for compounds to not contain aromatic rings, ergo increases of DBE 3 or more are often correlated within increasing aromaticity as it is unlikely that all the DBEs are saturated rings and double bonds. Additionally, increases in carbon number for any particular DBE value can be associated with increasing alkylation of a core structure (or several different core structures).

■ RESULTS AND DISCUSSION

Biocrude Properties. A comparison of the raw HTL biocrude fractions with the hydrotreated organic fractions is presented in Table 2. Generally, the bulk properties of the raw and hydrotreated pine HTL biocrude products are dissimilar to the microalgae and sewage sludge products, which in turn are similar in several respects. The CHNOS elemental analyses of the microalgae and sewage sludge raw biocrudes are relatively high at 1.6 H/C molar ratio due to the high concentration of lipid derivatives generated by hydrolysis of fats and oils. In contrast, the pine raw biocrude has a lower H/C ratio (0.97) reflective of a higher concentration of cyclic and oxygenated aromatic (e.g., phenolic) compounds. The higher concentrations of cyclic structures in the pine samples are derived from the lignin and starch in the original biomass. Lignin decomposes to a phenolic-rich stream, whereas cellulose has also been demonstrated to convert to oxygenated aromatics.[47] The cellulose present in the microalgae and sewage sludge samples also converts to oxygenated aromatics, but the total concentration of cyclics is lower due to the abundance of lipid-derived products. Another contrast between the microalgae and sewage sludge compared with the pine product is the elevated level of nitrogen and sulfur present in the microalgae and sewage sludge biocrudes. Nitrogen and sulfur in the microalgae and sewage sludge raw biocrudes are 20−30 times greater compared with pine due to the presence of proteins and, in the case of sulfur, polar lipids within the microalgae and sewage sludge feed materials. As proteins and carbohydrates degrade during HTL, N-heterocycles form through Maillard reactions.[46]

With hydrotreatment, all three biocrudes showed similar changes in their respective bulk properties. An increase of the carbon content (77−83 to 84−87%) and hydrogen content (6.7−11 to 11−15%) in the hydrotreated oils was observed (i.e., generation of pure hydrocarbons and others with reduced heteroatom content). A concurrent decrease in nitrogen (0.18−5.5 to <0.5%), oxygen (3.1−10 to 1.2−2%), and sulfur (<0.03−0.63 to <50 ppm) content indicated successful hydrodenitrogenation, hydrodeoxygenation, and hydrodesulfurization for all hydrotreated biocrudes. The density, viscosity, and moisture content of the hydrotreated biocrudes are lower than that of the raw biocrudes. Overall, the bulk property changes due to upgrading cause the hydrotreated biocrudes to have more in common with liquid petroleum liquid fuels and make them a more viable alternative fuel blendstock for refinery feedstock compared to their raw counterparts.

Simulated Distillation and GC-MS of Hydrotreated Biocrudes. Simulated distillation (Figure 1) and GC-MS

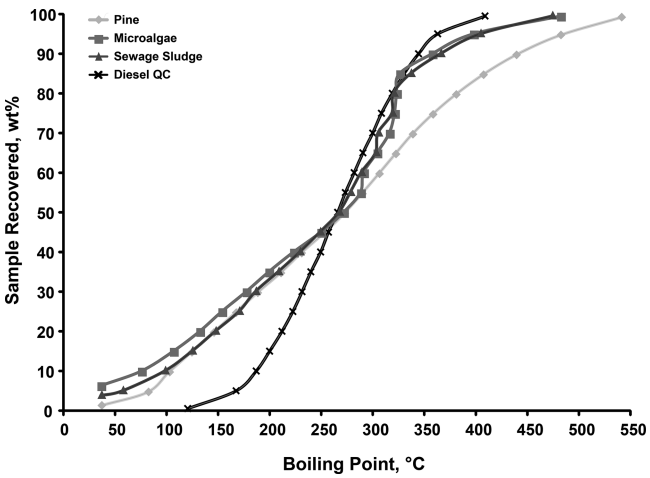

Figure 1. Simulated distillation profiles of the hydrotreated biocrudes from pine, microalgae, and sewage sludge feedstocks with a diesel QC sample included for comparison.

(Figure 2) of the hydrotreated samples again illustrate the general similarity of the *Chlorella* sp. microalgae and sewage sludge products and the contrast with the pine sample. From 35 to 260 °C, the distillation traces of all three products are relatively similar, which reflects the commonality of the naphthenic-rich light fractions in each sample. All three samples contain alkyl-substituted cycloalkanes with some open-chain hydrocarbons and alkyl benzenes also present. Above 260 °C, the amount of material distilled increases

DOI: 10.1021/acs.energyfuels.8b01445
Energy Fuels 2018, 32, 8483−8493

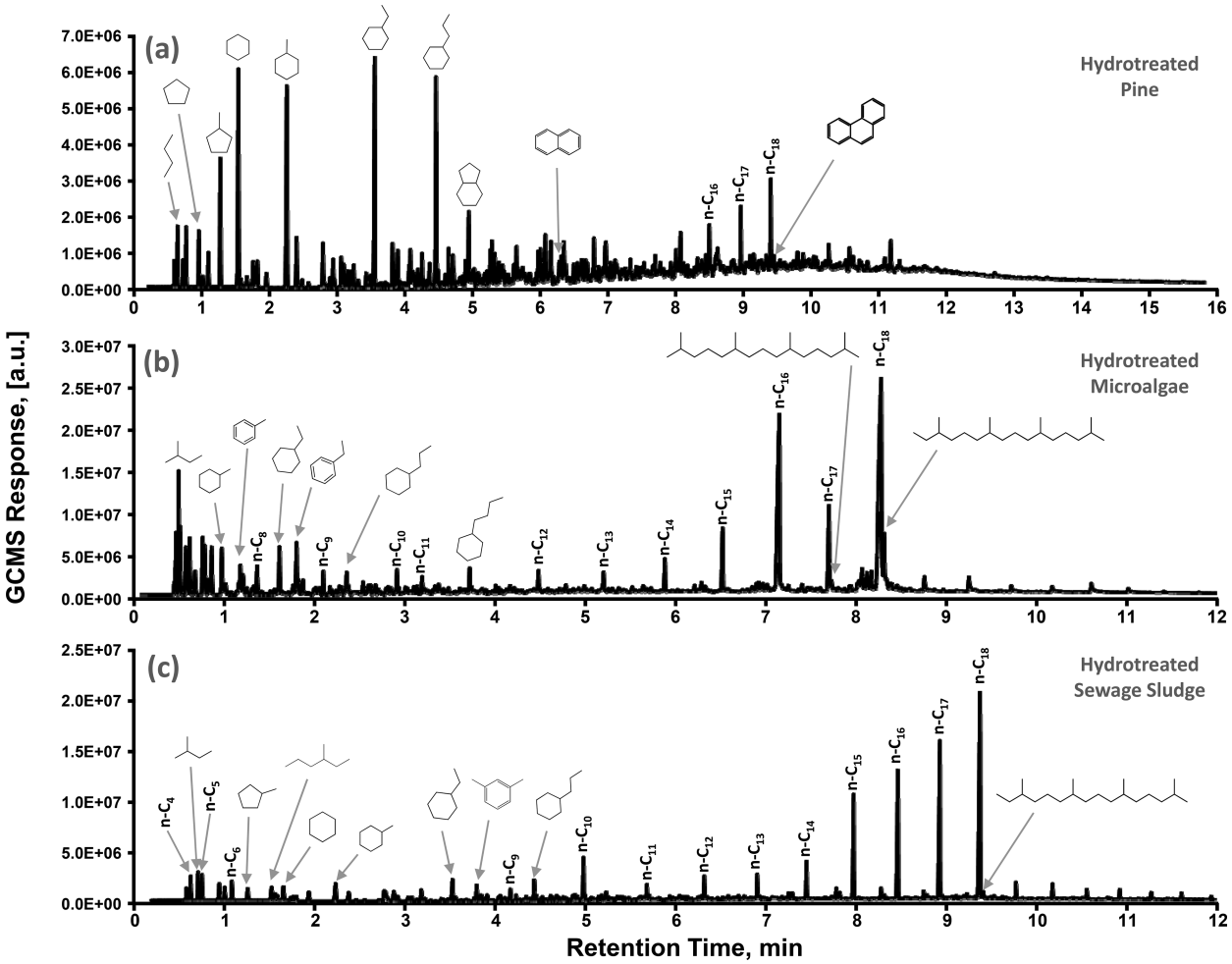

Figure 2. GC-MS of the hydrotreated pine (a), microalgae (b), and sewage sludge (c) biocrudes.

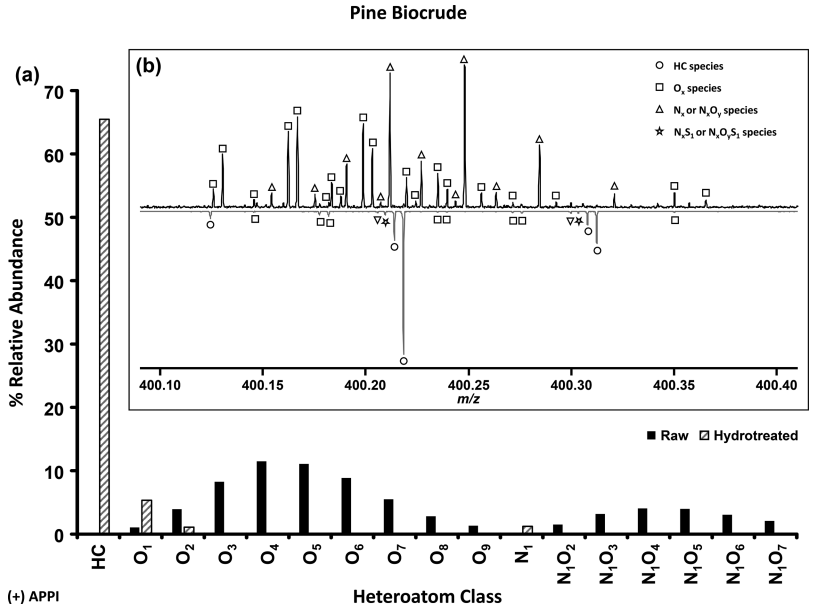

Figure 3. (a) Heteroatom class distributions derived from the (+) APPI mass spectra of the raw (solid) and hydrotreated (stripes) biocrude from pine feedstock. (b) Mass scale expanded segment at m/z 400 within the raw (solid, top) and hydrotreated (stripes, bottom) pine biocrude mass spectra.

sharply for the microalgae and sewage sludge products. The greatest proportion of material distilled between 260 and 350 °C for the microalgae and sewage sludge products derives from the high concentration of normal (n-) C15−C18 alkanes, from

DOI: 10.1021/acs.energyfuels.8b01445
Energy Fuels 2018, 32, 8483−8493

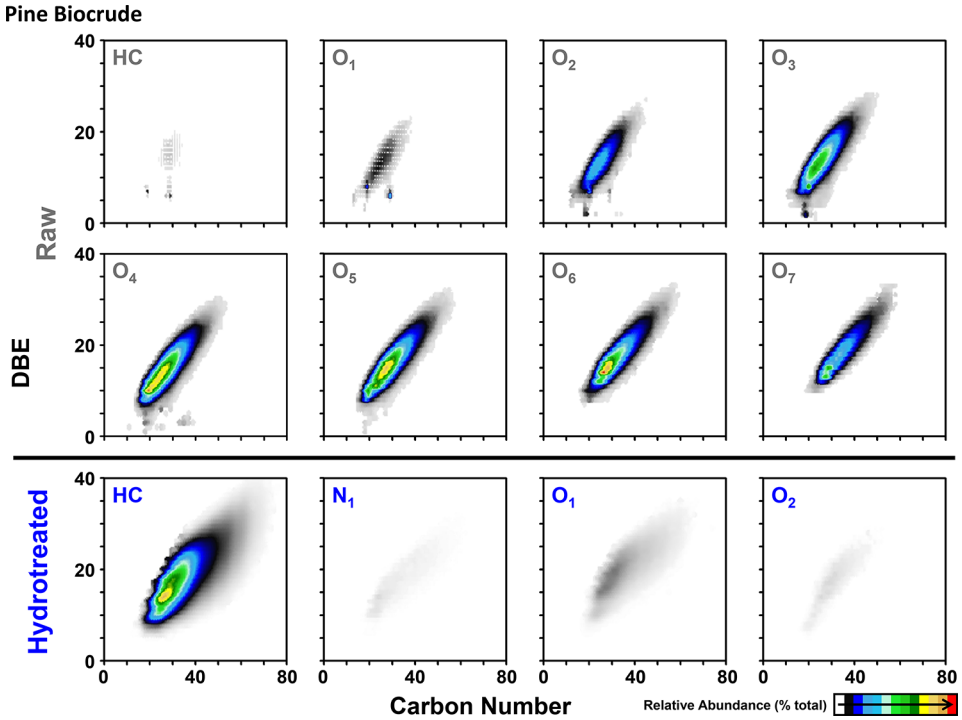

Figure 4. Isoabundance-contoured plots of DBE versus carbon number for the HC and O_{1-7} species derived from the (+) APPI mass spectra of the raw pine biocrude (top, gray) and the HC, N_1, O_1, and O_2 species derived from the (+) APPI mass spectra of the hydrotreated pine biocrude (bottom, blue). Plots are scaled to the most abundant peak in the mass spectrum.

lipids in the microalgae and sewage sludge feeds (which are shown by GC/MS to be primarily C16 and C18 lipids). The higher concentration of even-carbon number alkanes within the hydrotreated microalgae biocrude shows a preference for the complete reduction of the carboxyl group (i.e., loss of 2 carbons) over decarboxylation reactions (i.e., loss of 1 carbon). In contrast, whereas some *n*-C16 to *n*-C18 alkanes are present in the hydrotreated pine bio-oil, the concentration is lower overall compared to that of microalgae and sludge due to the low lipid content of the pine feedstock. Furthermore, a wider diversity of higher boiling compounds is present in the pine biocrude, as illustrated by the elevated baseline observed from 4.5 to 16 min retention time. The smooth simulated distillation profile for the hydrotreated pine biocrude also suggests the presence of a wide diversity of compounds. In contrast, the sharp increase in the sample recovered for the microalgae and sewage sludge illustrates the higher concentration of fewer *n*-alkanes. For the hydrotreated pine material, many of the compounds in the diesel boiling range are multicyclic and, in some cases, aromatic as determined by GC-MS. However, GC-MS can only show the composition of volatile, low molecular weight compounds; for example, FT-ICR MS has been employed to give a more detailed picture of the nonvolatile, higher molecular weight species present within the raw and hydrotreated HTL biocrudes.

FT-ICR MS Analysis. *Pine Biocrude.* The heteroatom class distributions derived from the (+) APPI mass spectra of raw and hydrotreated pine HTL biocrude are shown in Figure 3a. The species present within the raw pine biocrude range from O_{1-9} and N_1O_{2-9}, with each individual class consisting of <12% of the total relative abundance. During upgrading, deoxygenation reactions convert the high-oxygen-containing species from the parent biocrude to a more desirable product that is dominated by hydrocarbons (>65% relative abundance as measured by APPI FT-ICR MS) and contains <6% each of O_1, O_2, and N_1 species.

The mass scale expanded segments at m/z 400 within the (+) APPI mass spectra of raw and hydrotreated pine biocrudes help visualize the change that occurs to the raw biocrude due to hydrotreatment (mass spectral peak assignments can be found in Table S1). Of the 30 peaks present at m/z 400 (>10σ rms noise) within the raw biocrude, 19 of them are representative of O_x species and 12 are representative of nitrogen-containing species (Figure 3b, top). Upon upgrading, the total peaks present at m/z 400 (>10σ rms noise) dropped to 17. The most abundant peaks correspond to hydrocarbon species (5 in total) that were not present in the raw pine biocrude. Most of the abundant nitrogen-containing species from the raw biocrude have been converted to other compounds and are not present within the hydrotreated biocrude. The hydrotreated biocrude mass spectrum also contains several peaks representative of O_x species. Most of these peaks (O_x species) were present in the raw biocrude but are now present in lower relative abundance in the upgraded oil. Finally, the hydrotreated biocrude contains a few compounds that are representative of sulfur-containing compounds that were not present in the raw biocrude. It is difficult to determine if these peaks were generated during the hydrotreatment process or if they were present in the raw biocrude, albeit at concentrations below our limit of detection.

The isoabundance-contoured plots of DBE versus carbon number plots for various species from the raw and hydrotreated pine biocrude show compositional change due to the upgrading (Figure 4). The abundance (z-axis) for each of these plots is scaled to the most abundant species in each mass spectrum to illustrate which compounds are the dominant species observed in each sample. The raw biocrude shows several O_x species at high relative abundance, with the O_{3-7}

DOI: 10.1021/acs.energyfuels.8b01445
Energy Fuels 2018, 32, 8483−8493

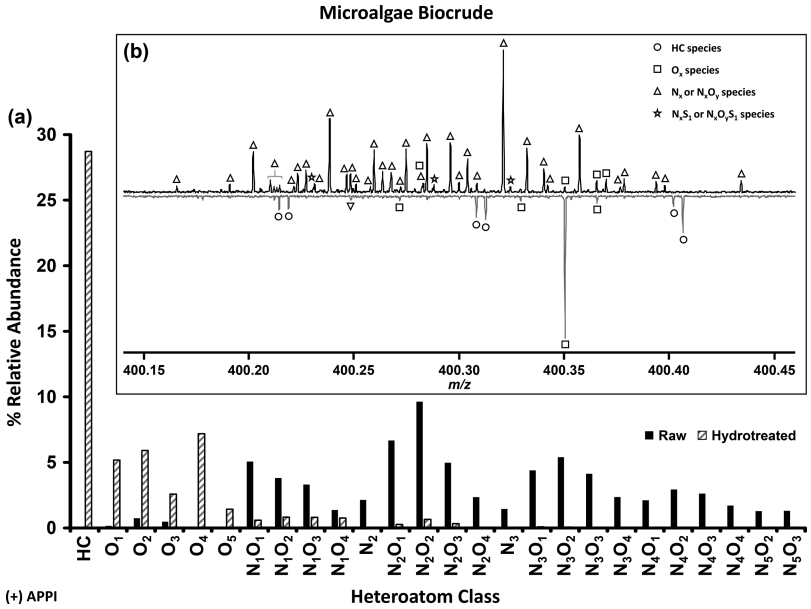

Figure 5. (a) Heteroatom class distributions derived from the (+) APPI mass spectra of the raw (solid) and hydrotreated (stripes) biocrude from microalgae feedstock. (b) Mass scale expanded segment at m/z 400 within the raw (solid, top) and hydrotreated (stripes, bottom) microalgae biocrude (+) APPI mass spectra.

classes each containing >5% relative abundance of all the species identified in the (+) APPI mass spectrum. The O_1 and hydrocarbon (HC) species are not abundant (<2%). In contrast, the hydrotreated pine biocrude APPI FT-ICR mass spectrum is dominated by hydrocarbon compounds that are substantially more abundant than the few N_1, O_1, and O_2 species that remain in the hydrotreated oil.

The hydrocarbon compounds in the raw pine biocrude range from C_{18-34} and DBE 5−20, whereas the hydrocarbon species within the hydrotreated biocrude range from C_{14-74} and DBE 6−40. Thus, comparison of the compositional space (C# and DBE) of the hydrotreated biocrude to that of the parent raw biocrude shows that most of the species within the HC class are new species generated through deoxygenation reactions. Additionally, the hydrotreated biocrude shows the creation of N_1 species that are not present in the raw biocrude. The hydrotreated O_1 species exist over a larger compositional space (i.e., C_{16-66} and DBE 6−36) than the species from the raw biocrude (i.e., C_{13-37} and DBE 3−22), with most of the new species having more aromatic character (DBE > 4) than the species in the raw biocrude. Finally, the lower abundance of the O_2 species and the higher abundance of the HC species in the hydrotreated oil compared to the higher abundance of the O_2 species (and higher O_x species) and lower abundance of the HC species in the raw biocrude demonstrates that the majority of species within the raw biocrude have been converted to pure hydrocarbons.

Microalgae Biocrude. The heteroatom class distributions derived from the (+) APPI mass spectra of raw and hydrotreated microalgae biocrude show the changes within the heteroatom classes due to upgrading (Figure 5a). Prior to hydrotreatment, the raw microalgae biocrude is composed mainly of nitrogen-containing classes ranging from $N_{1-5}O_{0-4}$. None of the heteroatom classes contains >10% of the total relative abundance. However, after hydrotreatment, the biocrude contains mostly HC (∼29%) species. The hydrotreated oil also contains O_1, O_2, and O_4 species in >5% relative abundance compared to the <1% relative abundance of these species in the untreated biocrude. Interestingly, the hydrotreated oil contains O_5 species, which are not present in the raw biocrude and were most likely generated during upgrading. Additionally, the hydrotreated oil contains $N_{1-2}O_{1-4}$ species, although in <1% relative abundance.

An analysis of the change in observed species at m/z 400 for the (+) APPI mass spectra of the raw and hydrotreated microalgae biocrude demonstrates the reduction in mass spectral complexity that accompanies upgrading (Figure 5b). The raw algae biocrude contains 44 peaks (>10σ rms noise) at m/z 400. Most of these peaks (37) belong to nitrogen- and nitrogen/oxygen-containing species. Within this region, only four peaks within the raw biocrude are representative of O_x species and another three belong to sulfur-containing species. In contrast, the hydrotreated oil only contains 11 peaks at m/z 400. Upon hydrotreatment, the number peaks representative of nitrogen- and nitrogen/oxygen-containing species is reduced to a single peak within this selected mass range. Six new peaks, which belong to hydrocarbon species, are now seen at m/z 400, indicative of hydrodenitrogenation to generate hydrocarbon species. Additionally, the hydrotreated oil contains four peaks which correspond to O_x species, with the peak at m/z 400.35030 ($C_{23}H_{47}O_4{}^{13}C_1$) being the most abundant and also present in the raw biocrude.

Figure S1 contains the isoabundance-contoured plots of DBE versus carbon number for the $N_{0-4}O_{1-3}$ species derived from the (+) APPI mass spectrum of raw microalgae biocrude. These plots are normalized to the most abundance species within each class to allow for easier visualization of the compositional space coverage of each class. Due to the higher nitrogen content of the algae feed, there are more species present in the nitrogen-containing classes from the raw biocrude than in the O_x classes. Most of the nitrogen-containing species range from C_{10-60} and DBE 1−25. Additionally, the species become more aromatic as the number of nitrogen atoms per molecule increases.

Conversely, the isoabundance-contoured plots of DBE versus carbon number for various classes from the hydro-

DOI: 10.1021/acs.energyfuels.8b01445
Energy Fuels 2018, 32, 8483−8493

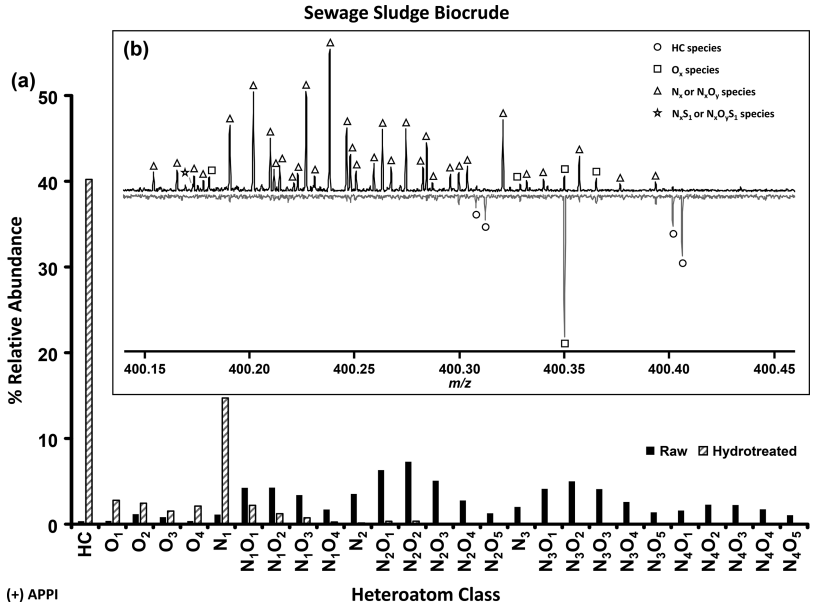

Figure 6. (a) Heteroatom class distributions derived from the (+) APPI mass spectra of the raw (solid) and hydrotreated (stripes) biocrude from sewage sludge feedstock. (b) Mass scale expanded segment at m/z 400 within the raw (solid, top) and hydrotreated (stripes, bottom) sewage sludge biocrude (+) APPI mass spectra.

treated microalgae biocrude show vastly different compositional space coverage compared to the raw biocrude (Figure S2). The blue outlines portray the limits of compositional space coverage present in the raw biocrude overlaid on the plots from the hydrotreated oil for ease of comparison. For all of the nitrogen-containing species, the compositional space covered by the species within the upgraded oil is greatly reduced from the raw biocrude. In the hydrotreated oil, most of the nitrogen-containing species from the raw biocrude have been converted, and the few remaining nitrogen species range from C_{8-20} and DBE 1−15. This suggests that most of the nitrogen-containing species have undergone hydrodeoxygenation and hydrodenitrogenation reactions to generate other species. Analysis of the DBE versus carbon number plots of the HC and O_{1-5} species in the hydrotreated algae oil compared to that of the raw algae biocrude shows increased compositional space coverage within each of these classes, indicative of the generation of new species. Similar to the nitrogen-containing species, several of the new O_x species are less alkylated than the original species present within the raw algae biocrude; however, the O_{2-4} species also contain a high relative abundance of new species which range from C_{30-50} and DBE 1−6, consistent with carboxylic, hydroxy, and dicarboxylic acids. Interestingly, the largest change in compositional space coverage occurs within the HC and O_1 classes. In the raw microalgae biocrude, these classes contain only a few compounds (mainly C_{18}, C_{23}, and C_{28} and DBE 2−10). However, in the hydrotreated algae biocrude, the HC species range from C_{10-60} and DBE 3−40 and the O_1 species range from C_{10-50} and DBE 1−35. Most of these new species generated during hydrotreatment are significantly more aromatic than the HC and O_1 species from the raw algae biocrude and possibly form from polymerization reactions.

Sewage Sludge Biocrude. The heteroatom class distributions derived from the (+) APPI mass spectra of raw and hydrotreated sewage sludge biocrude show change due to upgrading (Figure 6a). Prior to hydrotreatment, the raw biocrude shows HC and $N_{0-4}O_{0-5}$ species, with all of the classes consisting of <8% of the total relative abundance. After hydrotreatment, the resulting oil consists mainly of hydrocarbon species (∼40% relative abundance). The hydrotreated biocrude also contains a significant amount of N_1 species (∼15%) with the O_{1-4}, N_1O_{1-4}, and N_2O_{0-3} species each contributing <2% to the total relative abundance. These results suggest that the higher nitrogen- and oxygen-containing compounds present within the raw biocrude have undergone deoxygenation and denitrogenation reactions to generate molecules with lower heteroatom content as expected.

The mass scale expanded segments at m/z 400 for the (+) APPI mass spectra of raw and hydrotreated sewage sludge biocrudes depict compositional change that occurs due to hydrotreatment (Figure 6b). The biocrude contains 38 peaks (>10σ rms noise) at m/z 400, 33 of which belong to nitrogen-containing species, 4 that belong to O_x species, and 1 which corresponds a sulfur-containing species. In contrast, the hydrotreated biocrude only contains four peaks (>10σ rms noise) at m/z 400. Of these five peaks, four belong to hydrocarbon species which were not present in the raw biocrude and the other corresponds to an O_x compound that is present within raw biocrude, as well.

Figure S3 contains the isoabundance-contoured plots of DBE versus carbon number for the $N_{0-4}O_{1-3}$ species derived from the (+) APPI mass spectrum of raw sewage sludge biocrude. These plots are normalized to the most abundance species within each class. Similar to what is observed for the raw microalgae biocrude, there are more species present in the nitrogen-containing classes from the raw sewage sludge biocrude than in the O_x classes due to the high nitrogen content of the feed. Most of the nitrogen-containing species range from C_{10-60} and DBE 1−30 and are progressively more aromatic as the number of nitrogen atoms per molecule increases.

Alternatively, the isoabundance-contoured plots of DBE versus carbon number for various classes from the hydrotreated sewage sludge biocrude show different compositional space coverage compared to the raw biocrude (Figure S4).

DOI: 10.1021/acs.energyfuels.8b01445
Energy Fuels 2018, 32, 8483−8493

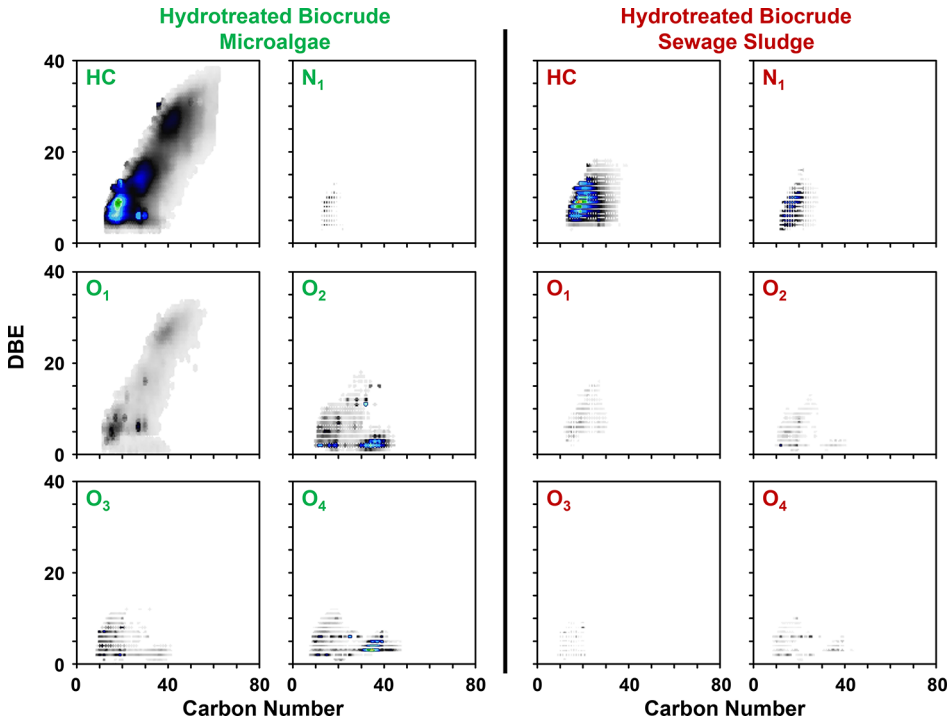

Figure 7. Isoabundance-contoured plots of DBE versus carbon number for the HC, N_1, and O_{1-4} species derived from the (+) APPI mass spectra of the hydrotreated microalgae (left, green) and sewage sludge (right, red) biocrudes. Plots are scaled to the most abundant peak in the mass spectrum.

Similar to the trends seen in the upgraded microalgae biocrude, the majority of the nitrogen-containing species present at higher carbon numbers and DBE values in the raw biocrude are not observed, and the few remaining compounds range from C_{10-20} and DBE 1−15. The compositional space of the O_{2-3} species does not change significantly between the raw and upgraded biocrude, ranging from C_{15-40} and DBE 1−15. In contrast to the hydrotreated microalgae biocrude, the HC and O_1 species in the hydrotreated sewage sludge biocrude do not extend to high DBE values and contain overall aromaticity similar to that of the species from the other classes within the hydrotreated oil.

Comparison of Hydrotreated Biocrudes. The isoabundance-contoured plots of DBE versus carbon number for HC, N_1, and O_{1-4} classes from the hydrotreated microalgae (left, green) and sewage sludge (right, red) biocrudes normalized to the most abundant species in the each spectrum are shown in Figure 7 for direct comparison of the most abundant classes from each hydrotreated biocrude. Both the hydrotreated algae and sewage sludge biocrudes are dominated by hydrocarbon species. However, the HC species present within the algae biocrude (DBE 3−40) are much more aromatic than the HC species present in the sewage sludge biocrude (DBE 3−20). More aromatic O_1 species are also present in the hydrotreated microalgae biocrude (DBE 1−35) relative to the sewage sludge biocrude (DBE 1−15). The more aromatic HC and O_1 species within the hydrotreated microalgae biocrude could suggest that polymerization or condensation reactions are more prevalent during the hydrotreatment of algae biocrudes than sewage sludge biocrudes. On the other hand, the hydrotreated sewage sludge contains a higher relative abundance and variety of N_1 species than the upgraded microalgae biocrude. The generation of more N_1 species during the hydrotreatment of the sewage sludge biocrude could indicate a higher occurrence of cracking reactions over polymerization reactions. In general, the O_{2-4} species within the microalgae and sewage sludge biocrude cover similar compositional space, ranging from C_{8-40} and DBE 1−20; however, these species appear to be more abundant in the hydrotreated algae biocrude, possibly due to more polymerization reactions.

The hydrotreated HC and O_1 species in the pine biocrude (HC = C_{14-74}, DBE 6−40; O_1 = C_{16-66}, DBE 6−36) cover a compositional space that is more similar to the hydrotreated microalgae biocrude (HC = C_{13-60}, DBE 3−40; O_1 = C_{10-50}, DBE 1−35) than the hydrotreated sewage sludge biocrude (HC = C_{13-39}, DBE 3−18; O_1 = C_{12-31}, DBE 2−16), which exhibit aromatic compounds (DBE > 20) (Figure S5). Interestingly, the HC species within the hydrotreated microalgae biocrude appear to consist of at least two separate distributions (i.e., DBE ∼ 3−20 and DBE ∼ 25−40), whereas the HC species within the hydrotreated pine biocrude constitute a single continuous distribution of species from DBE 6 to DBE 40. Possibly the HC species within the microalgae biocrude are generated from degradation of different types/structures of compounds with differing degrees of aromaticity, whereas the HC species within the pine biocrude are generated from more similar structures (e.g., lignin) and result in the more compositional similar HC species. The existence of different core structures within the hydrotreated microalgal and pine biocrudes is further corroborated by the presence of nonaromatic species (DBE < 4) within the microalgae biocrudes that are not present within the pine biocrude. Overall, the hydrotreated pine biocrude has a more aromatic character than either the hydrotreated microalgae or sewage sludge biocrudes, most likely due to the higher lignin and starch content of the lignocellulosic feed and the higher lipid content of the microalgae and sewage sludge feeds.

DOI: 10.1021/acs.energyfuels.8b01445
Energy Fuels 2018, 32, 8483−8493

Comparison of Hydrotreated HTL Biocrudes to Petroleum. The isoabundance-contoured plots of DBE versus carbon number for HC and N_1 species derived from the (+) APPI mass spectra of the hydrotreated pine (left), microalgae (middle), and sewage sludge (right) biocrudes are shown in Figure S5. These plots are normalized to the most abundant species in each spectrum. Overlaid on the DBE versus carbon number plots are the outlines of the compositional space covered by Gulf of Mexico (GOM) crude oil (red) and shale oil (green). A majority of hydrocarbon species present within the hydrotreated pine oil lie within the compositional space covered by the GOM crude oil. The major differences between the compositional space coverage of HC species within the sediment-derived oils and hydrotreated pine biocrude are (1) the hydrotreated pine biocrude contains fewer carbon numbers per any given DBE (i.e., less alkylated); (2) the hydrotreated pine biocrude contains less alkylated, more condensed core structures (i.e., compounds that lie to the left of the outlines and closer to the polyaromatic hydrocarbon (PAH) planar limit); and (3) the hydrotreated pine biocrude contains species with more aromaticity than seen in the organic-sediment derived oils (i.e., compounds above the outlines at higher DBE values). The HC species within the hydrotreated microalgae biocrude are less alkylated, more condensed, and more aromatic than sediment-derived oils. In contrast, the HC species within the hydrotreated sewage sludge biocrude are not as aromatic as HC species from the biomass-derived sources, containing less aromaticity than the GOM crude oil and similar aromaticity as the shale oil. Overall, the HC species within the upgraded sewage sludge biocrude cover similar compositional space as the shale oil but with slightly less alkylation (i.e., fewer carbon numbers per DBE value).

The N_1 species within the hydrotreated pine biocrude also follow similar trends as the HC species, with less alkylated, more condensed, and more aromatic compounds relative to the organic sediment-derived oils (Figure S5). However, the N_1 species from the hydrotreated microalgae and sewage sludge biocrude cover a much less diverse compositional space than either the upgraded pine biocrude or the organic sediment-derived oils, with species of relatively low carbon number (<30) and DBE values (<20).

The O_1 and O_2 species from the hydrotreated pine biocrude and the O_1 species from the hydrotreated microalgae biocrude also contain compounds which are less alkylated, more condensed, and more aromatic relative to the species from the organic sediment-derived oils (Figure S5). The O_1 species from the hydrotreated sewage sludge biocrude are less diverse than the GOM crude oil, ranging from C_{10-30} and DBE < 20, and contain lower carbon numbers than seen in the shale oil. The O_2 species from the hydrotreated algae and sewage sludge biocrudes contain compounds with DBE values lower than those seen in the organic sediment-derived oils. The nonaromatic O_2 species (i.e., DBE < 4) are more dominant in the microalgae and sewage sludge biocrudes due to their higher concentrations in these samples relative to the organic sediment-derived oils, in which the aromatic O_2 species are highlighted by (+) APPI.

CONCLUSION

Hydrotreatment of raw pine, microalgae, and sewage sludge biocrudes shows changes in bulk properties (i.e., increased hydrogen content, decreased nitrogen, oxygen, sulfur, and moisture content, and lower density and viscosity) that prove that hydrodenitrogenation, hydrodeoxygenation, and hydrodesulfurization reactions occurred to create more desirable products. Furthermore, GC-MS analysis of the hydrotreated biocrudes show that all three samples contain alkyl-substituted cycloalkanes with some open-chain hydrocarbons and alkyl benzenes also present. The hydrotreated microalgae and sewage sludge biocrudes show a greater concentration of *n*-alkanes, whereas the hydrotreated pine biocrude shows a lower concentration of *n*-alkanes and an overall larger diversity of compounds.

FT-ICR MS analysis reveals that raw pine biocrude is dominated by O_x species, whereas raw microalgae and sewage sludge biocrudes are dominated by N_xO_y species. After hydrotreatment, (+) APPI mass spectra of all three biocrudes show a significant reduction in mass spectral complexity (i.e., loss of O_x, N_x, and N_xO_y species) and a corresponding emergence of novel hydrocarbon species within the upgraded oils. Compositional space analysis of the raw and hydrotreated biocrude reveals the loss of higher (>2) heteroatom-containing species and the concurrent generation of hydrocarbon and lower heteroatom-containing species upon hydrotreatment, indicative of the species with the raw biocrudes undergoing hydrodeoxygenation, hydrodenitrogenation, and hydrodesulfurization reactions. Compared to organic sediment-derived oils, the hydrocarbons in all three hydrotreated biocrudes show reduced compositional complexity exhibited by less alkylated, more condensed core structures. The hydrocarbons within hydrotreated microalgae and sewage sludge biocrudes are more compositionally similar to shale oil, whereas hydrocarbons within the hydrotreated pine biocrude are more compositionally similar to a Gulf of Mexico crude oil.

Bulk property analyses, simulated distillation, GC-MS, and FT-ICR MS analysis of pine, microalgae, and sewage sludge biocrudes show striking similarities between the microalgae and sewage sludge biocrudes, which are often in contrast to the pine biocrude. The similarities between the microalgae and sewage sludge biocrudes can be attributed to higher concentrations of lipids, proteins, and cellulose in the feeds relative to the pine biocrude, which has a higher concentration of lignin and lower concentration of lipids.

ASSOCIATED CONTENT

Supporting Information

The Supporting Information is available free of charge on the ACS Publications website at DOI: 10.1021/acs.energyfuels.8b01445.

Elemental composition assignments for peaks at *m*/*z* 400 within the (+) APPI mass spectra of raw and hydrotreated pine, microalgae, and sewage sludge biocrudes (Table S1); isoabundance-contoured plots of DBE versus carbon number for various species derived from the (+) APPI mass spectra of the raw and hydrotreated microalgae and sewage sludge biocrudes (Figures S1−S4); isoabundance-contoured plots of double bond equivalents versus carbon number for the O_1 and O_2 species derived from the (+) APPI mass spectra of the hydrotreated pine (left), microalgae (middle), and sewage sludge (right) biocrudes (Figure S5) (PDF)

DOI: 10.1021/acs.energyfuels.8b01445
Energy Fuels 2018, 32, 8483−8493

AUTHOR INFORMATION

Corresponding Author

*Phone: +1 575 646 5156. Fax: +1 575 646 1597. E-mail: tschaub@nmsu.edu.

ORCID

Karl O. Albrecht: 0000-0003-0465-4864

Tanner M. Schaub: 0000-0002-5747-4237

Notes

The authors declare no competing financial interest.

ACKNOWLEDGMENTS

This work was supported by the U.S. Department of Energy's Office of Energy Efficiency and Renewable Energy thought the Bioenergy Technologies Office, the United States National Science Foundation (IIA-1301346), the Center for Animal Health and Food Safety at New Mexico State University, and NSF Division of Materials Research (DMR-11-57490). Pacific Northwest National Laboratory (PNNL) is operated by Battelle Memorial Institute for the DOE under Contract No. DE-AC05-76RL01830. The authors thank the ICR staff at National High Magnetic Field for the use of the FT-ICR MS facility and assistance with instrument configuration and data collection. The authors also kindly acknowledge contributions from Richard Lucke at PNNL for performing the simulated distillation and GC-MS analysis of the hydrotreated biocrude samples.

REFERENCES

(1) Elliott, D. C.; Biller, P.; Ross, A. B.; Schmidt, A. J.; Jones, S. B. Hydrothermal Liquefaction of Biomass: Developments from Batch to Continuous Process. *Bioresour. Technol.* **2015**, *178*, 147−156.

(2) Elliott, D. C.; Hart, T. R.; Schmidt, A. J.; Neuenschwander, G. G.; Rotness, L. J.; Olarte, M. V.; Zacher, A. H.; Albrecht, K. O.; Hallen, R. T.; Holladay, J. E. Process Development for Hydrothermal Liquefaction of Algae Feedstocks in a Continuous-Flow Reactor. *Algal Res.* **2013**, *2* (4), 445−454.

(3) Davis, R. E.; Fishman, D. B.; Frank, E. D.; Johnson, M. C.; Jones, S. B.; Kinchin, C. M.; Skaggs, R. L.; Venteris, E. R.; Wigmosta, M. S. Integrated Evaluation of Cost, Emissions, and Resource Potential for Algal Biofuels at the National Scale. *Environ. Sci. Technol.* **2014**, *48* (10), 6035−6042.

(4) Toor, S. S.; Rosendahl, L.; Rudolf, A. Hydrothermal Liquefaction of Biomass: A Review of Subcritical Water Technologies. *Energy* **2011**, *36* (5), 2328−2342.

(5) Biddy, M.; Davis, R.; Jones, S.; Zhu, Y. *Whole Algae Hydrothermal Liquefaction Technology Pathway: Technical Report*; NREL/TP-5100-58051; PNNL-22314; U.S. Department of Energy: Washington, D.C., 2013.

(6) Jarvis, J. M.; Billing, J. M.; Hallen, R. T.; Schmidt, A. J.; Schaub, T. M. Hydrothermal Liquefaction Biocrude Compositions Compared to Petroleum Crude and Shale Oil. *Energy Fuels* **2017**, *31*, 2896.

(7) Hossain, F. M.; Rainey, T. J.; Ristovski, Z.; Brown, R. J. Performance and Exhaust Emissions of Diesel Engines Using Microalgae FAME and the Prospects for Microalgae HTL Biocrude. *Renewable Sustainable Energy Rev.* **2018**, *82*, 4269.

(8) Lavanya, M.; Meenakshisundaram, A.; Renganathan, S.; Chinnasamy, S.; Lewis, D. M.; Nallasivam, J.; Bhaskar, S. Hydrothermal Liquefaction of Freshwater and Marine Algal Biomass: A Novel Approach to Produce Distillate Fuel Fractions through Blending and Co-Processing of Biocrude with Petrocrude. *Bioresour. Technol.* **2016**, *203*, 228−235.

(9) Gerber, L. N.; Tester, J. W.; Beal, C. M.; Huntley, M. E.; Sills, D. L. Target Cultivation and Financing Parameters for Sustainable Production of Fuel and Feed from Microalgae. *Environ. Sci. Technol.* **2016**, *50* (7), 3333−3341.

(10) Zhu, Y.; Biddy, M. J.; Jones, S. B.; Elliott, D. C.; Schmidt, A. J. Techno-Economic Analysis of Liquid Fuel Production from Woody Biomass via Hydrothermal Liquefaction (HTL) and Upgrading. *Appl. Energy* **2014**, *129*, 384−394.

(11) Huber, G. W.; Corma, A. Synergies between Bio-and Oil Refineries for the Production of Fuels from Biomass. *Angew. Chem., Int. Ed.* **2007**, *46* (38), 7184−7201.

(12) Speight, J. G. In *Handbook of Petroleum Analysis*; Winefordner, J. D., Ed.; Wiley-Interscience: New York, 2001.

(13) Biller, P.; Sharma, B. K.; Kunwar, B.; Ross, A. B. Hydroprocessing of Bio-Crude from Continuous Hydrothermal Liquefaction of Microalgae. *Fuel* **2015**, *159*, 197−205.

(14) Pedersen, T. H.; Jensen, C. U.; Sandström, L.; Rosendahl, L. A. Full Characterization of Compounds Obtained from Fractional Distillation and Upgrading of a HTL Biocrude. *Appl. Energy* **2017**, *202*, 408−419.

(15) Marshall, A. G.; Rodgers, R. P. Petroleomics: The Next Grand Challenge for Chemical Analysis. *Acc. Chem. Res.* **2004**, *37* (1), 53−59.

(16) Hsu, C. S.; Hendrickson, C. L.; Rodgers, R. P.; McKenna, A. M.; Marshall, A. G. Petroleomics: Advanced Molecular Probe for Petroleum Heavy Ends. *J. Mass Spectrom.* **2011**, *46* (4), 337−343.

(17) McKenna, A. M.; Nelson, R. K.; Reddy, C. M.; Savory, J. J.; Kaiser, N. K.; Fitzsimmons, J. E.; Marshall, A. G.; Rodgers, R. P. Expansion of the Analytical Window for Oil Spill Characterization by Ultrahigh Resolution Mass Spectrometry: Beyond Gas Chromatography. *Environ. Sci. Technol.* **2013**, *47* (13), 7530−7539.

(18) Schaub, T. M.; Jennings, D. W.; Kim, S.; Rodgers, R. P.; Marshall, A. G. Heat-Exchanger Deposits in an Inverted Steam-Assisted Gravity Drainage Operation. Part 2. Organic Acid Analysis by Electrospray Ionization Fourier Transform Ion Cyclotron Resonance Mass Spectrometry. *Energy Fuels* **2007**, *21* (1), 185−194.

(19) Purcell, J. M.; Merdrignac, I.; Rodgers, R. P.; Marshall, A. G.; Gauthier, T.; Guibard, I. Stepwise Structural Characterization of Asphaltenes during Deep Hydroconversion Processes Determined by Atmospheric Pressure Photoionization (APPI) Fourier Transform Ion Cyclotron Resonance (FT-ICR) Mass Spectrometry †. *Energy Fuels* **2010**, *24* (4), 2257−2265.

(20) Corilo, Y. E.; Rowland, S. M.; Rodgers, R. P. Calculation of the Total Sulfur Content in Crude Oils by Positive-Ion Atmospheric Pressure Photoionization Fourier Transform Ion Cyclotron Resonance Mass Spectrometry. *Energy Fuels* **2016**, *30*, 3962.

(21) Juyal, P.; Mapolelo, M. M.; Yen, A.; Rodgers, R. P.; Allenson, S. J. Identification of Calcium Naphthenate Deposition in South American Oil Fields. *Energy Fuels* **2015**, *29* (4), 2342−2350.

(22) Klein, G. C.; Angström, A.; Rodgers, R. P.; Marshall, A. G. Use of Saturates/Aromatics/Resins/Asphaltenes (SARA) Fractionation To Determine Matrix Effects in Crude Oil Analysis by Electrospray Ionization Fourier Transform Ion Cyclotron Resonance Mass Spectrometry. *Energy Fuels* **2006**, *20* (2), 668−672.

(23) Smith, D. F.; Schaub, T. M.; Kim, S.; Rodgers, R. P.; Rahimi, P.; Teclemariam, A.; Marshall, A. G. Characterization of Acidic Species in Athabasca Bitumen and Bitumen Heavy Vacuum Gas Oil by Negative-Ion ESI FT−ICR MS with and without Acid−Ion Exchange Resin Prefractionation. *Energy Fuels* **2008**, *22* (4), 2372−2378.

(24) Rowland, S. M.; Robbins, W. K.; Corilo, Y. E.; Marshall, A. G.; Rodgers, R. P. Solid-Phase Extraction Fractionation To Extend the Characterization of Naphthenic Acids in Crude Oil by Electrospray Ionization Fourier Transform Ion Cyclotron Resonance Mass Spectrometry. *Energy Fuels* **2014**, *28* (8), 5043−5048.

(25) Lobodin, V. V.; Robbins, W. K.; Lu, J.; Rodgers, R. P. Separation and Characterization of Reactive and Non-Reactive Sulfur in Petroleum and Its Fractions. *Energy Fuels* **2015**, *29* (10), 6177−6186.

(26) Lobodin, V. V.; Nyadong, L.; Ruddy, B. M.; Curtis, M.; Jones, P. R.; Rodgers, R. P.; Marshall, A. G. DART Fourier Transform Ion Cyclotron Resonance Mass Spectrometry for Analysis of Complex Organic Mixtures. *Int. J. Mass Spectrom.* **2015**, *378*, 186.

DOI: 10.1021/acs.energyfuels.8b01445
Energy Fuels 2018, 32, 8483−8493

(27) Faeth, J. L.; Jarvis, J. M.; McKenna, A. M.; Savage, P. E. Characterization of Products from Fast and Isothermal Hydrothermal Liquefaction of Microalgae. *AIChE J.* **2016**, *62*, 815.
(28) Sudasinghe, N.; Dungan, B.; Lammers, P.; Albrecht, K.; Elliott, D.; Hallen, R.; Schaub, T. High Resolution FT-ICR Mass Spectral Analysis of Bio-Oil and Residual Water Soluble Organics Produced by Hydrothermal Liquefaction of the Marine Microalga Nannochloropsis Salina. *Fuel* **2014**, *119*, 47−56.
(29) Sudasinghe, N.; Cort, J. R.; Hallen, R.; Olarte, M.; Schmidt, A.; Schaub, T. Hydrothermal Liquefaction Oil and Hydrotreated Product from Pine Feedstock Characterized by Heteronuclear Two-Dimensional NMR Spectroscopy and FT-ICR Mass Spectrometry. *Fuel* **2014**, *137*, 60−69.
(30) Jarvis, J. M.; Sudasinghe, N. M.; Albrecht, K. O.; Schmidt, A. J.; Hallen, R. T.; Anderson, D. B.; Billing, J. M.; Schaub, T. M. Impact of Iron Porphyrin Complexes When Hydroprocessing Algal HTL Biocrude. *Fuel* **2016**, *182*, 411−418.
(31) Lopez Barreiro, D.; Prins, W.; Ronsse, F.; Brilman, W. Hydrothermal Liquefaction (HTL) of Microalgae for Biofuel Production: State of the Art Review and Future Prospects. *Biomass Bioenergy* **2013**, *53*, 113−127.
(32) Sanguineti, M. M.; Hourani, N.; Witt, M.; Sarathy, S. M.; Thomsen, L.; Kuhnert, N. Analysis of Impact of Temperature and Saltwater on Nannochloropsis Salina Bio-Oil Production by Ultra High Resolution APCI FT-ICR MS. *Algal Res.* **2015**, *9*, 227−235.
(33) Cheng, F.; Cui, Z.; Chen, L.; Jarvis, J.; Paz, N.; Schaub, T.; Nirmalakhandan, N.; Brewer, C. E. Hydrothermal Liquefaction of High- and Low-Lipid Algae: Bio-Crude Oil Chemistry. *Appl. Energy* **2017**, *206*, 278−292.
(34) Zhang, J.; Qian, C.; Jiang, B. Bio-Crude Production via Hydrothermal Liquefaction of Enteromorpha Prolifera: Operating Condition Optimization and High Resolution FT-ICR Mass Spectral Analysis. *J. Agric. Saf. Health* **2017**, *60*, 1799−1806.
(35) Oasmaa, A.; Kuoppala, E.; Elliott, D. C. Development of the Basis for an Analytical Protocol for Feeds and Products of Bio-Oil Hydrotreatment. *Energy Fuels* **2012**, *26*, 2454−2460.
(36) Elliott, D. C. Historical Developments in Hydroprocessing Bio-Oils. *Energy Fuels* **2007**, *21* (3), 1792−1815.
(37) Snowden-Swan, L.; Zhu, Y.; Jones, S.; Elliott, D.; Schmidt, A.; Hallen, R.; Billing, J.; Hart, T.; Fox, S.; Maupin, G. *Hydrothermal Liquefaction and Upgrading of Municipal Wastewater Treatment Plant Sludge: A Preliminary Techno-Economic Analysis*; PNNL-25464; Richland, WA, 2016.
(38) Marrone, P. A. *Genifuel Hydrothermal Processing Bench-Scale Technology Evaluation Project*; WE&RF Report LIFT6T14; London, UK, 2016.
(39) Elliott, D. C.; Wang, H.; French, R.; Deutch, S.; Iisa, K. Hydrocarbon Liquid Production from Biomass via Hot-Vapor-Filtered Fast Pyrolysis and Catalytic Hydroprocessing of the Bio-Oil. *Energy Fuels* **2014**, *28* (9), 5909−5917.
(40) Kaiser, N. K.; Quinn, J. P.; Blakney, G. T.; Hendrickson, C. L.; Marshall, A. G. A Novel 9.4 T FTICR Mass Spectrometer with Improved Sensitivity, Mass Resolution, and Mass Range. *J. Am. Soc. Mass Spectrom.* **2011**, *22*, 1343−1351.
(41) Blakney, G. T.; Hendrickson, C. L.; Marshall, A. G. Predator Data Station: A Fast Data Acquisition System for Advanced FT-ICR MS Experiments. *Int. J. Mass Spectrom.* **2011**, *306* (306), 246−252.
(42) Kaiser, N. K.; Savory, J. J.; McKenna, A. M.; Quinn, J. P.; Hendrickson, C. L.; Marshall, A. G. Electrically Compensated Fourier Transform Ion Cyclotron Resonance Cell for Complex Mixture Mass Analysis. *Anal. Chem.* **2011**, *83*, 6907−6910.
(43) Ledford, E. B., Jr.; Rempel, D. L.; Gross, M. L. Space Charge Effects in Fourier Transform Mass Spectrometry Mass Calibration. *Anal. Chem.* **1984**, *56*, 2744−2748.
(44) Corilo, Y. E. *PetroOrg*; Florida State University; www.petroorg.com.
(45) Kendrick, E. A Mass Scale Based on CH2 = 14.0000 for High Resolution Mass Spectrometry of Organic Compounds. *Anal. Chem.* **1963**, *35*, 2146−2154.
(46) Kumar, G.; Shobana, S.; Chen, W.-H.; Bach, Q.-V.; Kim, S.-H.; Atabani, A. E.; Chang, J.-S. A Review of Thermochemical Conversion of Microalgal Biomass for Biofuels: Chemistry and Processes. *Green Chem.* **2017**, *19* (1), 44−67.
(47) Nelson, D. A.; Molton, P. M.; Russell, J. A.; Hallen, R. T. Application of Direct Thermal Liquefaction for the Conversion of Cellulosic Biomass. *Ind. Eng. Chem. Prod. Res. Dev.* **1984**, *23* (3), 471−475.

DOI: 10.1021/acs.energyfuels.8b01445
Energy Fuels 2018, 32, 8483−8493